Journal of Spacecraft and Rockets
Vol. 44, No. 6, November–December 2007

Neutral Density Measurements from the Gravity Recovery and Climate Experiment Accelerometers

Byron D. Tapley,* John C. Ries,† Srinivas Bettadpur,‡ and Minkang Cheng§
University of Texas at Austin, Austin, Texas 78759

DOI: 10.2514/1.28843

Predicting the orbits of space objects in low-altitude orbits requires an accurate model for the atmospheric neutral density. The current accuracy of semi-empirical models limits the prediction accuracy and impacts a number of operational decisions. The current models are based on sparse measurements of the neutral density, collected over an extended period. One of the problems is observing the thermosphere density changes in response to the solar and geomagnetic variability on short temporal scales, such as those characterized by geomagnetic storms. The stochastic behavior of the solar forcing represents one of the major challenges in predicting satellite orbits. In situ measurements of the density can play a significant role in improving the structure of the neutral density models and in providing a timely measurement for enhancing the accuracy of the satellite predictions. Measurements from orbiting accelerometers carried by the twin Gravity Recovery and Climate Experiment satellites have the potential for providing accurate and timely measurements to improve the satellite prediction accuracy. The objective of this paper is to describe the procedure for using the Gravity Recovery and Climate Experiment accelerometer measurements for determining accurate density measurements.

Nomenclature

A_k = area for the kth satellite surface
A_u = astronomical unit
$\boldsymbol{B}(t)$ = constant and variable accelerometer environmental influences
$\boldsymbol{B}^*$ = estimated accelerometer bias
$\boldsymbol{b}, \dot{\boldsymbol{b}}, \ddot{\boldsymbol{b}}$ = vector offset of proof mass from satellite center of mass and its time derivatives
C_{Dk} = atmospheric drag coefficient for the kth surface
C_{dif} = diffuse reflectivity coefficient for the satellite surface element
C_{Lk} = atmospheric lift coefficient for the kth surface
C_{spc} = specular reflectivity coefficient for the satellite surface element
$\boldsymbol{D}$ = atmospheric drag acceleration
$\mathrm{d}A$ = satellite surface element
f_d = atmospheric drag scale factor
$\boldsymbol{f}_d$ = other disturbing influences on the accelerometer proof mass
$\boldsymbol{f}_{\mathrm{exc}}$ = accelerometer sensor unit excitations
$\boldsymbol{f}_{\mathrm{ng}}$ = satellite nongravitational accelerations
$\boldsymbol{f}_{\mathrm{obs}}$ = accelerometer measurement
$\boldsymbol{f}_{\mathrm{true}}$ = estimate of true nongravitational accelerations
$\boldsymbol{G}(\boldsymbol{f}_{\mathrm{exc}})$ = accelerometer nonlinear response to input excitations
m = satellite mass
$\boldsymbol{n}$ = unit vector normal to the satellite surface element
$\boldsymbol{n}_k$ = normal direction for the kth satellite surface
$\boldsymbol{n}(t)$ = accelerometer measurement noise
R = distance to the sun
$\boldsymbol{R}_s$ = satellite position vector in the inertial system
S = estimated accelerometer scale matrix (assumed diagonal)
$\boldsymbol{S}$ = unit vector to the sun
S_f = solar flux constant
$\boldsymbol{V}$ = satellite velocity with respect to the atmosphere
$\boldsymbol{V}_a$ = atmosphere velocity
$\boldsymbol{V}_s$ = satellite velocity in inertial system
$\boldsymbol{V}_w$ = thermospheric wind velocity
Γ = gravity gradient matrix at the accelerometer proof mass
ρ = atmospheric density
$\Sigma(t)$ = accelerometer nonorthogonality matrix
Ω_E = Earth's rotation rate
$\boldsymbol{\Omega}_E$ = Earth's angular velocity
$\boldsymbol{\omega}, \dot{\boldsymbol{\omega}}$ = satellite angular velocity and angular acceleration
ω_a = atmosphere rotation rate
$\wedge$ = ratio of the atmosphere rotation rate to the Earth's rotation rate

Presented as Paper 6171 at the 2006 AIAA/AAS Astrodynamics Specialist Conference, Keystone, CO, 21–24 August 2006; received 15 November 2006; revision received 30 March 2007; accepted for publication 10 May 2007.

*Director and Professor, Center for Space Research, 3925 West Braker Lane, Suite 200. Member AIAA.

†Senior Research Scientist, Center for Space Research, 3925 West Braker Lane, Suite 200.

‡Senior Research Scientist, Center for Space Research, 3925 West Braker Lane, Suite 200. Member AIAA.

§Research Scientist, Center for Space Research, 3925 West Braker Lane, Suite 200.

I. Introduction

CHANGES in the density and composition of the neutral atmosphere create variations in the drag effects on the low-Earth orbiters (LEO), and these effects must be carefully accounted for in LEO mission predictions for maneuver planning, reentry prediction, collision hazard avoidance, risk analysis, and tracking of objects in space using narrow-field-of-view sensors. Existing empirical density models used for these purposes lack the spatial and temporal resolution to account for dynamic changes in the neutral density. The discrepancies between models and observations appear, in particular, at high latitudes, in which there is extreme variability in the electric field and aurora particle precipitation. To increase the accuracy and the spatial and temporal resolution of density values for drag computations, the U.S. Air Force Space Command's High-Accuracy Satellite Drag Model (HASDM) [1] has emerged, which uses the analysis of the evolution of the trajectories of 60–75 LEO spacecraft to obtain real-time corrected density calculations. The availability of data from accelerometers onboard LEO missions offers great potential for the improvement of such density-modeling efforts. Two missions presently carry accelerometers in low-Earth orbit. The Challenging Minisatellite Payload (CHAMP) [2] is an Earth-gravity and magnetic field mapping mission, launched in 2000 by the DLR, German Aerospace Research Center into a near-500-km, 87-deg inclination orbit. The joint NASA/DLR Gravity Recovery and Climate Experiment (GRACE) [3] is an Earth-gravity mapping mission launched in March 2002, with twin satellites in 89-deg inclination, coplanar, 500-km-alt orbits, separated by 220 km along the track. The initial altitude has decreased over the course of their more than five-year mission lifetimes. Each of the three satellites carries a high-accuracy accelerometer (ACC) to measure the nongravitational force on the satellite, which, for their respective orbit altitudes, is predominantly atmospheric drag. The accelerometers onboard the GRACE satellites are well suited to the purposes of density-model improvements. The instruments have demonstrated stable performance over their four years in orbit, and the data have demonstrated extraordinary precision in the measurement of the accelerations due to the nongravitational forces. Furthermore, the availability of two identical instruments offers a means of cross validation and blunder detection for the two sets of density estimates. The effects of the neutral winds and atmosphere rotation are a part of the signals contained in the accelerometer data. Separation of the effects of the meridional winds, in particular, will lead to improved determination of the neutral density and to advances in the understanding of the Earth's thermospheric dynamic response to the insertion of energy and momentum.

II. Accelerometer Application to Density Investigations

The importance of accelerometer measurements has been shown from the analysis of the miniature electrostatic accelerometer (MESA) accelerometer data [4,5] and the spatial triaxial accelerometer for research (STAR) from CHAMP [6]. The GRACE mission uses a more accurate version of the STAR (SuperSTAR) on each of two satellites, which orbit in the same plane separated by a nominal distance of 220 km. The accurate measurements of the nongravitational accelerations of the GRACE satellites can also provide a critical assessment of the currently used nongravitational force models. The drag model is specified by the reference atmospheric density and the drag coefficient, and the former indirectly affects the determination of the density from ACC data. The drag coefficient, as a measure of gas-surface interaction, is a key component, for which the uncertainty is the dominant error source in the derived density from ACC data. The use of the accelerometer data for density determination is based upon a good understanding and accounting for those error sources. The purpose of this presentation is to describe the methodology for analyzing the ACC data from the two GRACE satellites and its use in the determination of the neutral atmospheric density at the GRACE satellite altitudes.

A. Accelerometer Analysis Methodology

The processing of the accelerometer data to obtain accurate neutral density and thermospheric wind fields is a complicated process dominated by four essential components. The first of these components is the accurate calibration of the raw accelerometer data. At present, the processed accelerometer products are tailored for gravity-field-determination applications. The accelerometer data must be reprocessed for the unique needs of the aeronomy applications. The second is the development of accurate surface area and interaction models for the effects of solar and Earth radiation pressure effects acting on GRACE satellites. Removal of solar and Earth radiation effects from the accelerometer data is required to avoid aliasing both long-wavelength and episodic artifacts (such as shadow-crossing effects) into the resulting atmospheric products. The third addresses the role of the satellite lift and drag coefficients, and the fourth lies in the determination of the atmospheric rotation and wind.

The SuperSTAR accelerometer outputs are obtained by a sensor unit (SU) based on the measurements of the analog voltages that provide the electrostatic forces needed to maintain the proof-mass suspension at the center of a cage. The analog signals from the SU are digitized through a Butterworth filter by the instrument control unit (ICU). The net force, or the "excitation" of the sensor unit, is composed of many effects, which can be written as

$$\boldsymbol{f}_{\text{exc}} = \boldsymbol{f}_{\text{ng}} + \boldsymbol{\omega} \times \boldsymbol{\omega} \times \boldsymbol{b} + \dot{\boldsymbol{\omega}} \times \boldsymbol{b} + 2\boldsymbol{\omega} \times \dot{\boldsymbol{b}} + \ddot{\boldsymbol{b}} - \Gamma \boldsymbol{b} + \boldsymbol{f}_d \tag{1}$$

The first term on the right is the sum of all the nongravitational acceleration signals, including atmospheric drag, Earth and solar radiation pressure, and residual thrust accelerations from the firing of the attitude control and maneuvering jets. The next four terms are the proof-mass motion in a satellite-fixed rotating frame attached to the accelerometer, but for which the origin is offset from the satellite center of mass by the vector $\boldsymbol{b}$ ($\dot{\boldsymbol{b}}$ and $\ddot{\boldsymbol{b}}$ are the first and second time derivatives). The GRACE mission controls this magnitude to be less than 100 μm, small enough that the rotational accelerations can be neglected. This assumption is not necessarily valid for other satellite accelerometers. The body-fixed axis rotates with the angular velocity $\boldsymbol{\omega}$ and angular acceleration $\dot{\boldsymbol{\omega}}$ of the satellite. The 3×3 matrix Γ represents the matrix of the gradients of gravity at the accelerometer proof mass. Finally, $\boldsymbol{f}_d$ represents the vector of the remaining disturbing influences on the accelerometer proof mass relative to its electrode cage, but which do not contribute to a change in linear momentum of the spacecraft (e.g., structural influences).

The digital data by the ICU are delivered at a 10-Hz rate. The process of making measurements with a noisy instrument, along with the associated environmental effects, allows the instrument output to be represented as

$$\boldsymbol{f}_{\text{obs}} = \boldsymbol{B}(t) + \Sigma(t)\boldsymbol{f}_{\text{exc}} + \boldsymbol{G}(\boldsymbol{f}_{\text{exc}}) + \boldsymbol{n}(t) \tag{2}$$

where $\boldsymbol{B}(t)$ is the sum of a (constant) bias and variable environmental influences such as thermal variability of the instrument. The 3×3 matrix $\Sigma(t)$ contains scale factors along its diagonals and represents the nonorthogonality of the proof mass and electrode cage with its off-diagonal elements. This matrix may also be time-dependent due to environmental influences. The third term denotes the small nonlinearity of the response of the accelerometer to its input excitation and is neglected in the following analysis. The last term denotes measurement noise. Finally, the ground data processing converts the raw 10-Hz measurements into the so-called GRACE level-1B data products [7] at a 1-Hz rate. The primary characteristics of the SuperSTAR payload on the GRACE satellites are summarized in Table 1.

The accelerometer measurements from GRACE are not absolute measurements of the nongravitational forces acting on the spacecraft. The true acceleration due to the nongravitational force on the spacecraft is modeled as

$$\boldsymbol{f}_{\text{true}} = \boldsymbol{B}^{*} + S\boldsymbol{f}_{\text{obs}} \tag{3}$$

where $\boldsymbol{B}^{*}$ is a modeled offset in the measured acceleration $\boldsymbol{f}_{\text{obs}}$ in the three orthogonal accelerometer axes, and S is a 3×3 matrix with its diagonal elements used to scale elements of $\boldsymbol{f}_{\text{obs}}$. Because $\boldsymbol{f}_{\text{true}}$ and the gravitational acceleration drive the motion of the satellite in space, the bias and scale factor must be determined as part of fitting the satellite orbit to the tracking data. This is accomplished during the operational GRACE gravity-field determination [3]. The biases for three components were solved in one-day intervals and the scale factors were solved monthly to obtain a more stable separation of the bias and scale factors. Figures 1 and 2 show the daily bias and

Table 1 SuperSTAR performance specifications

Measurement bandwidth	$\sim$3 Hz within the range 10^{-4} Hz and 40 mHz
Dynamic range	Nominal mode: ± 50 μm/s^2 in Y/Z; ± 500 μm/s^2 in X (cross-track)
Linear acceleration output	10-Hz rate, 24-bit conversion (10^{-11} m/s^2 precision in Y/Z)
Angular accel output	1-Hz rate, 24-bit conversion
Housekeeping	10-s output of critical proof-mass voltage and position measurements; 60-s output of SU and ICU temperatures

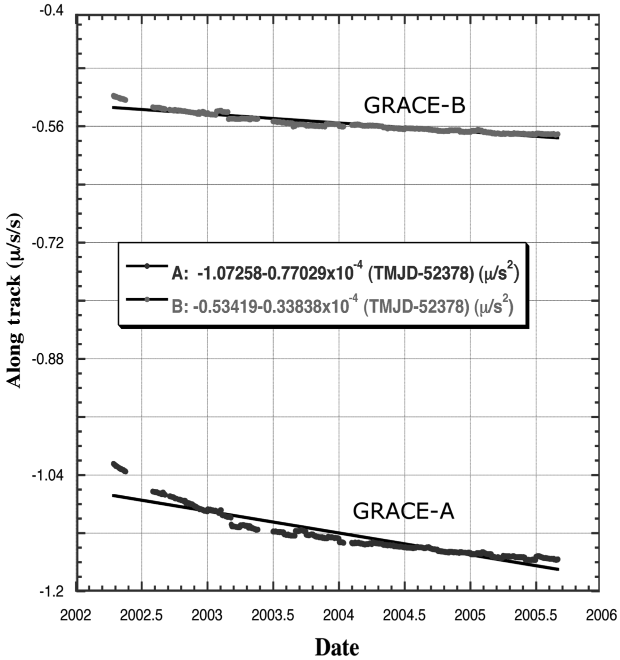

Fig. 1 Estimated bias for along-track accelerometer data.

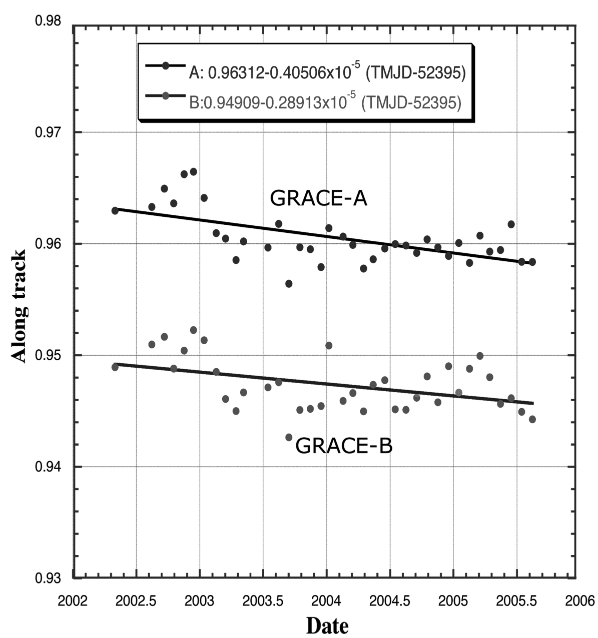

Fig. 2 Estimated scale factor for along-track accelerometer data.

monthly scale factor estimates for the along-track accelerations for GRACE-A and GRACE-B from the GRACE monthly gravity solutions. The regression coefficients from a linear fit to the daily bias and monthly scale estimates were used to scale and remove the bias for the level-1B GRACE ACC data in the density determination. The rms after the linear fit is less than $0.006/\mathrm{s}^2$ for the bias and 0.002 for the scale for both satellites. The accelerometer instruments are identical for GRACE-A and GRACE-B, but the system biases are different. The scale estimated from the gravity solutions appears to be variable from one month to another, and there is a clear change in character in both the scale and bias time series occurring in early 2003. In future analyses, the linear regression will be split into separate intervals.

After applying the bias and scale factors, the accelerometer data represent the best estimate of the total surface forces acting on the spacecraft. These include atmospheric drag, solar and Earth radiation pressure, and episodic thrusting events associated with the imbalances in the attitude control system. In the analysis here, the level-1B products were meant for gravity processing, and so the thrusting events had to be retained. By design, there are no thrusters in the along-track direction, and so the effect of these thruster imbalances is relatively small for this component. They are considerably larger for the cross-track component, which affects the recovery of the zonal winds from the accelerometer data. In addition, the high rate data (10 Hz) were filtered and sampled down to 1 Hz. To retain density variations occurring at shorter time scales, the original unfiltered 10-Hz data would have to be processed.

To extract the atmospheric density from these measurements of the surface forces, the effect of radiation pressure must be subtracted and a model for the relationship between the drag acceleration and the atmosphere density must be employed. The models for the radiation pressure and the atmospheric drag are described in the following section.

B. Models for the Drag Acceleration

The atmospheric drag acceleration on a satellite is expressed as

$$\boldsymbol{D} = -\frac{1}{2}\cdot\rho\cdot\sum_{k=1}^{6}\frac{A_k}{m}[C_{Dk}(\boldsymbol{V}\cdot\boldsymbol{n}_k)\boldsymbol{V} + C_{Lk}(\boldsymbol{V}\times\boldsymbol{n}_k)\times\boldsymbol{V}] \tag{4}$$

where

$$\boldsymbol{V} = \boldsymbol{V}_s - \boldsymbol{V}_a \qquad \boldsymbol{V}_a = \wedge(\boldsymbol{R}_s\times\boldsymbol{\Omega}_E) + \boldsymbol{V}_w \tag{5}$$

A_k and $\boldsymbol{n}_k$ are the area and normal direction of the corresponding kth surface defined in the satellite body-fixed system (only five of the six surfaces are involved at any time); $\boldsymbol{V}$ is the velocity of the satellite with respect to the atmosphere velocity, defined as $\boldsymbol{V} = \boldsymbol{V}_s - \boldsymbol{V}_a$, where $\boldsymbol{V}_s$ and $\boldsymbol{V}_a = \wedge(\boldsymbol{R}_s\times\boldsymbol{\Omega}_E) + \boldsymbol{V}_w$ are the velocity of the spacecraft and atmosphere in the inertial system, respectively; $\boldsymbol{R}_s$ is the position vector of the satellite; $\wedge$ is the ratio of the atmosphere rotation rate ω_a to the Earth's rotation rate Ω_E defined as ω_a/Ω_E; $\boldsymbol{\Omega}_E$ is the Earth's angular velocity; and $\boldsymbol{V}_w$ is the thermospheric wind. The satellite mass m (in kilograms) and time (in modified Julian date format (TMJD) is modeled as $m = 482.6\text{-}0.0061\times$ (TMJD-52850) for GRACE-A and $m = 484.69\text{-}0.0038\times$ (TMJD-52850) for GRACE-B.

The calculation of atmospheric drag with Eq. (4) requires the determination of the drag and lift coefficients C_{Dk} and C_{Lk}. These can be estimated using GPS or other tracking of the satellite, but to do so involves adopting an a priori density model, and the separation of the mean density from the parameter estimates is not possible [8]. These coefficients can also be determined from physical models, as described next.

At high altitude, in which the atmosphere is assumed to be in thermal diffusive equilibrium, the aerodynamic force is the net momentum delivered to the satellite surface by the incident and reflected molecules. The drag and lift coefficients are a measure of the gas–surface interaction. The total momentum striking a flat surface of unit area in the normal and tangential direction can be computed [9] based on the assumption that the free-molecular flow through a uniform gas in equilibrium and with a Maxwellian distribution of velocity. The major uncertainty is the modeling of the momentum carried away from the surface by the emitted molecules. Experiments have shown that the character of the reemission depends on the temperature at the satellite surface. A number of models were proposed and examined in the past several decades. These models include the Schamberg model [10] and the Nocilla model [11]. The Nocilla model has been reported to fit the majority of the reflected velocity distributions that were observed in molecular beam experiments [12]. Because of its simplicity and popularity, the Schamberg model was used for the calculations of the drag and lift coefficients. However, the uncertainty of the drag coefficient from this model may not be predictable to better than 10%, which must be taken into account in determination of the density from ACC data. With the applied atmospheric density model and the ratio of the effective area-to-mass ratio known with sufficient accuracy, a scale factor f_d for the drag (and lift) force was adjusted over a selected time interval to best fit the GRACE tracking data. The estimated scale factor f_d is used to make the model best fit the actual atmospheric drag that the GRACE satellite experienced. The three-year mean of the f_d estimates accounts principally for systematic error in modeling the drag coefficient and can used as a calibration factor for the drag coefficients to determine the density from ACC data.

C. Solar Radiation Pressure Modeling

The model used for calculating the effects of the solar radiation pressure is a critical component in separating the atmospheric drag from the overall surface forces. The radiation force on a satellite is the net momentum per unit time exchanged between the satellite surface and sunlight (or Earthlight). The radiation force acting on the element surface dA of the satellite can be expressed as follows [13]:

$$\mathrm{d}\boldsymbol{F} = -S_f\left[\frac{A_u}{R}\right]^2[(1 - C_{\mathrm{spc}})\boldsymbol{S} + 2(C_{\mathrm{dif}}/3 + C_{\mathrm{spc}}\cos\theta)\boldsymbol{n}]\frac{\mathrm{d}A}{m}|\cos\theta| \tag{6}$$

where $\boldsymbol{S}$ and $\boldsymbol{n}$ are the unit vectors for the satellite to the sun and normal direction of the satellite surface; m is the mass of the satellite; S_f is the solar flux constant; A_u is the astronomical unit; R is the distance to the sun; C_{spc} and C_{dif} are the specular and diffuse reflectivity coefficient of the surface, respectively; and $\cos\theta = \boldsymbol{n}\cdot\boldsymbol{S}$.

Because the solar flux is nearly constant, the modeling of the radiation force depends on the accuracy of the effective cross-sectional area and the reflection properties of the various satellite surfaces. The latter are specified by the coefficients of the absorption, specular, and diffuse reflection coefficients (the ratio of the absorbed or reflected momentum of the satellite surface to the incident momentum carried by sunlight). In the current orbit computations, the radiation acceleration force is evaluated for each individual surface, with the area and absorption or reflectivity coefficients specified in the GRACE product specifications [14], but the uncertainty in these values is unknown in the space environment. In addition, the spacecraft structure is currently represented by a small number of simple surfaces, whereas the actual surfaces are more complicated and consist of several different materials. Consequently, efforts are required to improve both the calculation of the radiation pressure forces for a better determination of the density and, especially, for studies of the wind field from the cross-track accelerometer data.

III. Discussion of Results

Figures 3 and 4 show a comparison of acceleration magnitude from the various models for the various surface forces acting on the GRACE-A satellite for the along-track (Fig. 3) and cross-track (Fig. 4) directions. The radial component of the ACC data is not used for determining the density. The results span four orbital revolutions on 5 November 2004. The model effects for the drag and the solar radiation pressure are shown as individual components. The drag component is from the 1978 drag-temperature model (DTM78) [15] density model. Drag clearly dominates the along-track component, but the contribution from radiation pressure is not negligible and must be accurately modeled before removal. The large contributions of radiation pressure to the radial and cross-track components can be used in calibrating the radiation pressure model. Note that the along-track acceleration is relatively free from the accelerations associated with the attitude control system thrusting. However, the cross track has large impulsive accelerations, which must be removed to obtain an accurate estimate of the cross-track drag and wind-induced acceleration. Note the influence of the rapid change in the radiation pressure as the satellite goes into the Earth-shadowed region. The model for the radiation pressure must be accurate, because the entrance into shadow occurs near the poles, in which there is considerable interest in other rapidly varying atmospheric phenomena. Throughout most of the sunlit periods, the radiation pressure is a significant fraction of the drag acceleration.

Figure 5 compares the density recovered for a quiet day (1 August 2002) with the atmospheric density calculated using the DTM78 and the 1971 Jacchia (J71) [16] density models, in which a mean adjustment was made to allow comparison with the variations. The time interval covers a little over two orbital revolutions. As expected, the agreement between density estimates from GRACE-A and GRACE-B is generally much better than the agreement with the models. For the data span shown, the agreement with DTM78 is better than with the J71 model. These density models predict only the smooth or slowly changing components of the atmospheric density variations. The results indicate that the GRACE accelerometer data provide an important measurement for improvement in modeling of density variations at the GRACE altitude. In addition, the difference between the density variations measured by two GRACE satellites, separated by ~200 km, will reveal the interesting spatial features

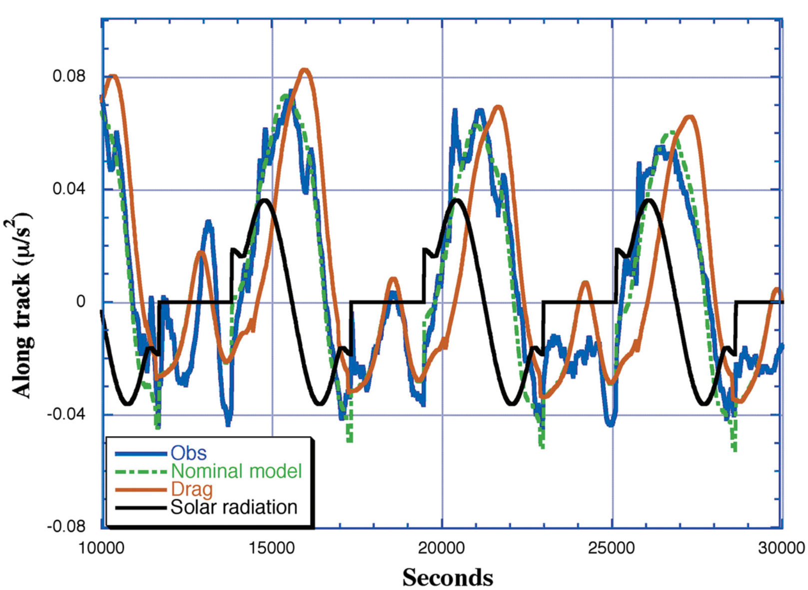

Fig. 3 GRACE accelerometer data and comparison with surface force models for the along-track component on 5 November 2004. The nominal model is the sum of the models for drag and solar radiation pressure.

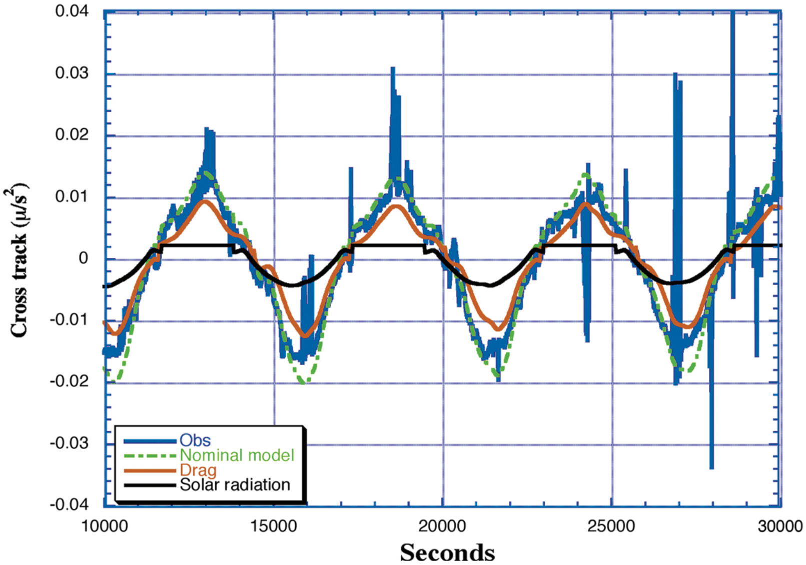

Fig. 4 GRACE accelerometer data and comparison with surface force models for the cross-track component on 5 November 2004. The nominal model is the sum of the models for drag and solar radiation pressure.

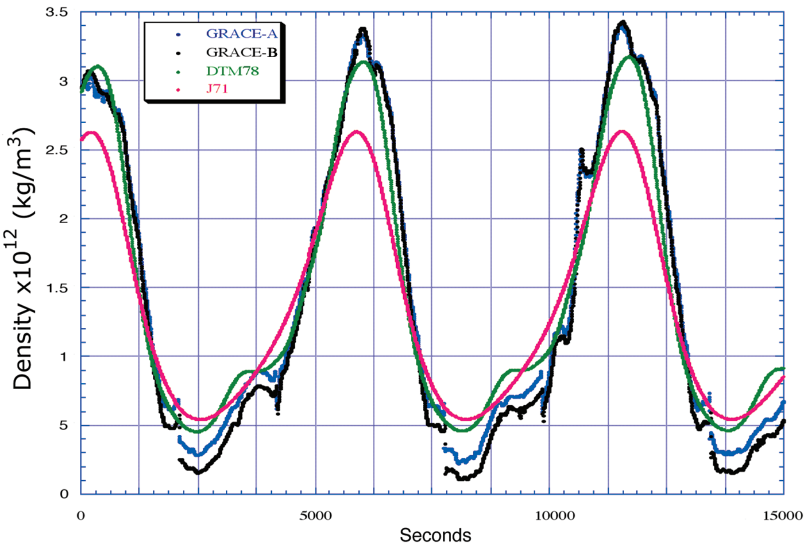

Fig. 5 Atmospheric density determined from GRACE accelerometer data on 1 August 2002 compared with density models.

with density variations at a resolution of a few hundreds of kilometers.

IV. Conclusions

Accurately determining the neutral density from satellite accelerometer measurements requires the following:

1) The scale factor and biases for each accelerometer axis must be determined and the data must be aligned with inertial space.

2) Artifacts (thrusts, twangs, etc.) must be removed or filtered.

3) Surface forces other than atmospheric drag must be accurately modeled and removed from total nongravitational accelerations observed by the accelerometer.

4) The model of the drag force must accurately represent the interaction between the atmosphere and the spacecraft surfaces to infer density.

Following this procedure, the accelerometer data from the twin-satellite GRACE mission were analyzed to derive the total atmospheric neutral density. Although some models appear to fairly well represent the smooth or slowly changing components of the atmospheric density, very dramatic departures from the models are observed in the GRACE data.

It was noted previously that the accuracy of the calculated atmospheric density is limited by the uncertainties in the ballistic coefficient, atmosphere rotation rate, and upper atmospheric winds, as well as the calibration parameters (bias and scale factor) for the accelerometer data. For GRACE, the accelerometer parameters are generally well-determined (typically, better than 0.01 μ/s^2) and contribute very little to the error. The uncertainty of the drag coefficient could be 5 to 10% or more [17].

Acknowledgment

This study was supported by the U.S. Air Force Office of Scientific Research under grant FA9550-06-1-0061.

References

[1] Storz, M. F., Bowman, B. R., and Branson, M. J. I., "High Accuracy Satellite Drag Model (HASDM)," AIAA Paper 2002-4886, 2002.

[2] Reigber, Ch., Schwintzer, P., and Lühr, H., "The CHAMP Geopotential Mission," *Bollettino di Geofisica Teorica e Applicata*, Vol. 40, Nos. 3–4, 1999, pp. 285–289.

[3] Tapley, B., Bettadpur, S., Watkins, M., and Reigber, Ch., "The Gravity Recovery and Climate Experiment: Mission Overview and Early

Results," *Geophysical Research Letters*, Vol. 31, No. 9, 2004, p. L09607.
doi:10.1029/2004GL019920

[4] Marcos, F. A., and Swift, E. R., "Application of the Satellite Trixial Accelerometer Experiment to Atmospheric Density and Wind Study," U.S. Air Force Geophysics. Lab., Rept. TR-82-0091, Hanscom AFB, MA, 1982.

[5] Marcos, F. A., and Forbes, J. M., "Thermospheric Winds from the Satellite Electronic Triaxial Accelerometer System," *Journal of Geophysical Research*, Vol. 90, July 1985, pp. 6543–6552.

[6] Biancale, R., Perosanz, F., Lemoine, J.-M., Sarailh, M., Bruinsma, S., and Loyer, S., "STAR Accelerometer Data Processing and Results, Part 1," *Advances in the Astronautical Sciences*, Vol. 109, 2001, pp. 467–478.

[7] Case, K., Kruizinga, G. L. H., and Wu, S. C., "GRACE Level 1B Data Product User Handbook JPL D-22027," ftp://podaac.jpl.nasa.gov/pub/grace/doc/Handbook_1B_v1.2.pdf [retrieved 30 Mar. 2007].

[8] Sengoku, A., Cheng, M. K., and Schutz, B. E., "Anisotropic Reflection Effects on Satellite Ajisai," *Journal of Geodesy*, Vol. 70, No. 3, 1995, pp. 140–145.
doi:10.1007/BF00943689

[9] Cook, G. E., "Satellite Drag Coefficients," *Planetary and Space Science*, Vol. 13, Oct. 1965, pp. 929–946.
doi:10.1016/0032-0633(65)90150-9

[10] Schamberg, R., "A New Analytic Representation," The Rand Corp., Rept. RM-2313, Santa Monica, CA, 1959.

[11] Nocilla, S., "The Surface Re-Emission Law in Free Molecule Flow," *Rarefied Gas Dynamics*, edited by J. A. Laurmann, Vol. 1, Academic Press, New York, 1963, pp. 327–346.

[12] Gregory, J. C., and Peter, P. N., "A Measurement of the Angular Distribution of 5 eV Atomic Oxygen Scattered Off a Solid Surface in Earth Orbit," *Rarefied Gas Dynamics*, edited by V. Boffi and C. Cercignani, Vol. 2, B. G. Teubner, Stuttgart, Germany, 1987, pp. 644–654.

[13] Milani, A., Nobili, A., and Farinella, P., *Non-Gravitational Perturbations and Satellite Geodesy*, Adam Hilger, Bristol, England, U.K., 1987, pp. 49, 125.

[14] Bettadpur, S., "GRACE 327-720 (CSR-GR-03-02)," http://podaac.jpl.nasa.gov/grace/documentation.html [retrieved 20 Mar 2007].

[15] Barlier, F., Berger, C., Fallin, J. L., Kockarts, G., and Thuillier, G., "A Thermospheric Model Based on Satellite Drag," *Annales de Géophysique*, Vol. 34, No. 1, 1978, pp. 9–24.

[16] Jacchia, L. G., "Revised Static Models of the Thermosphere and Exosphere with Empirical Temperature Profiles," *Smithsonian Astrophysical Observatory Special Report* Rept. 332, Cambridge, MA, 1971.

[17] Bruinsma, S., and Biancale, R., "STAR Accelerometer Data Processing and Results, Part 2," *Advances in the Astronautical Sciences*, Vol. 109, 2001, pp. 479–492.

A. Ketsdever
Associate Editor